

(8, 9) to stem-group animals and crown-group Eumetazoa (4, 10, 11). The recent general consensus is that these fossils are polyphyletic (12, 13): at least some members of the Ediacara biota are almost unanimously interpreted as bilaterian animals (*Kimberella*) (14, 15), while others are confidently ascribed to giant protozoa (*Palaeopascichnus*) (16). *Beltanelliformis*, although previously interpreted as bacteria, benthic and planktonic algae, as well as different animals, is now recognized as a spherical colony of cyanobacteria based on their biomarker content (17). The affinity of most other Ediacarans however remains controversial even at the Kingdom level (4). Most recently, arguments surrounding these fossils have centred on lichens, giant protists and stem- or crown group Metazoa.

10

While the lichen hypothesis (7) requires an implausible re-interpretation of the habitat of the Ediacara biota from a marine to a continental depositional environment (18), for many Ediacaran fossils, including dickinsoniids, it currently seems impossible to distinguish between giant protist and metazoan origins (4, 19). Some Ediacaran fossils, such as *Palaeopascichnus*, were likely giant unicellular eukaryotes (protists) (16), which means that, in contrast to modern ecosystems, these organisms were present, and sometimes extremely abundant, in shallow-water Ediacaran habitats (20). Features of dickinsoniids such as ‘quilting’ patterns, the inferred absence of dorso-ventral differentiation, and putative external digestion mode were found to be compatible with modern giant protists and hard to reconcile with metazoans (8, 20). Some modern giant protists can be up to 25 cm in size (21). In the absence of metazoan competition they may have become even larger, thereby possibly providing an explanation for the size range of Ediacaran protistan fossils (8). Some giant protists even have a motile lifestyle, compatible with Ediacaran trace fossils (22) and dickinsoniid ‘footprints’ (15). For dickinsoniids, the absence of evidence for a mouth and gut, perceived absence of bilateral symmetry and possible external digestion are all consistent with a protistan origin. However, all of the above characteristics are also compatible with basal Metazoa such as the Placozoa that are situated at the very base of Eumetazoa (23), while rejection of an external digestion mode and acceptance of supposed cephalization (15) may place dickinsoniids even higher on the metazoan tree. The nature of dickinsoniids, and most other Ediacaran fossils, thus remains unresolved.

30

We applied a novel approach (17) to test the lichen, protist and animal hypotheses by studying biomarkers extracted from organically preserved dickinsoniids. Hydrocarbon biomarkers are the molecular fossils of lipids and other biological compounds. Encased in sedimentary rock, biomarkers may retain information about their biological origins for hundreds of millions of years. For instance, hopanes are the hydrocarbon remains of bacterial hopanepolyols, while saturated steranes and aromatic steroids are diagenetic products of eukaryotic sterols. The most common sterols of Eukarya possess a cholesterol, ergosteroid or stigmasteroid skeleton with 27, 28 or 29 carbon atoms respectively. These C₂₇ to C₂₉ sterols, distinguished by the alkylation pattern at position C-24 in the sterol side chain, function as membrane modifiers and are widely distributed across extant Eukarya, but their relative abundances can give clues about the source organisms (24).

45

Apart from *Dickinsonia* (Fig. 1B), which is one of the most recognizable Ediacaran fossils, dickinsoniids include *Andiva* (Extended Data Fig. 1C), *Vendia*, *Yorgia* and other flattened Ediacaran organisms with segmented metameric bodies and a median line along the

body axes, separating the ‘segments’. The specimens for this study were collected from two surfaces in the Lyamtsa (*Dickinsonia*) and Zimnie Gory (*Andiva*) localities of the Ediacara biota in the White Sea region (Russia). Both *Dickinsonia* and *Andiva* are preserved in negative hyporelief on the sole of sandstones with microbial mat impressions and consist of a thin (up to around 3 μm) film of organic matter. The organic matter was detached from the rock surface (Fig. S1) and extracted for hydrocarbon biomarkers under strict exclusion of contamination (see Methods). Much thinner organic films covering the surfaces around *Andiva* fossils from the Zimnie Gory locality were extracted as well, providing a background signal coming from associated microbial mats. Investigation of biomarker composition of surrounding surfaces and enclosing sedimentary rocks allowed not only to subtract the background signal, but also to make sure that the biomarker signal from the fossils is not contaminated (Supplementary Text) Biomarkers were analysed using gas chromatography-mass spectrometry (see Methods).

The deposits immediately above and below *Dickinsonia* are characterized by a monoaromatic steroid distribution of 10.6–11.9% cholesteroloids, 13.4–16.8% ergosteroids and 71.3–76.0% stigmateroids, consistent with the general steroid distribution of sediments at the Lyamtsa locality (Fig. 1). The strong stigmateroid predominance is typical for the Ediacaran period and presumably related to green algae (Chlorophyta) inhabiting benthic mats or the water column (25). In these and all other Ediacaran sediment samples from the White Sea region, the carbon-number distribution of saturated steranes is nearly identical to the distribution of monoaromatic steroid homologues and always dominated by green algal stigmateroids (Table 1). In stark contrast, biomarkers extracted from the isolated organic matter of the largest *Dickinsonia* specimen had a monoaromatic steroid distribution of 93% cholesteroloids, 1.8% ergosteroids and 5.2% stigmateroids (Table 1, Fig. 1A). A general trend of increasing monoaromatic cholesteroloid abundance from 84.8% to 93.0% from the smaller to the larger *Dickinsonia* specimens (Fig. 1D), reflects decreasing contribution of the green algal background signal (Fig. S2).

The striking abundance of cholesteroloids in *Dickinsonia* is corroborated by an unusual sterane isomer distribution. In sediments surrounding the fossils in Lyamtsa and Zimnie Gory localities, the ratio of 5β over 5α stereoisomers for all steranes is generally near the equilibrium diagnostic for abiological isomerization (average $5\beta/5\alpha = 0.65 \pm 0.26$, $n = 54$, Figs. 1D,E). By contrast, in the fossils, $5\beta/5\alpha$ of cholestane is markedly elevated, up to 5.5 in *Dickinsonia* (Table 1, Figs. 1C,D,E), values that are generated by strictly anaerobic microbial activity (26, 27) such as during the decay of carcasses. Though gut flora of some mammals are known to produce 5β -stanols (precursors of 5β -steranes) (28), high relative abundance of these molecules in some background sediments (Fig. 1E) and macroalgae (17) from the White Sea contests the otherwise exciting possibility that 5β -steranes originated from *Dickinsonia*’s gut microbiota (see Supplementary Text). Notably, 5β ergostanes and stigmastanes in the *Dickinsonia* extracts are not elevated (Table 1), demonstrating that they are ultimately not derived from dickinsoniids but from the underlying microbial mat or surrounding sediment (Fig. S2). Based on these steroid homologue and isomer patterns, we compute that the sterols of living *Dickinsonia* consisted of at least 99.7% cholesteroloids (Supplementary Information). Within analytical precision, it is impossible to exclude that *Dickinsonia* produced traces of ergosteroids (up to 0.23%) or stigmateroids (up to 0.07%). Such steroids, if present, may be

derived from the organism itself, but could also represent dietary uptake or contributions from symbionts.

5 Biomarker signatures of *Andiva* specimens from the Zimnie Gory locality are less well differentiated from the microbial mat background signal and do not display a clear elevation of cholesteroloids relative to the background (Table 1). Yet, even in these fossils, $5\beta/5\alpha$ ratios for cholestanes are significantly higher ($5\beta/5\alpha = 1.02\text{--}1.31$) when compared to ergostanes and stigmastanes from the fossil extract ($5\beta/5\alpha = 0.52\text{--}0.66$) and the surrounding mat ($5\beta/5\alpha = 0.65\text{--}0.81$; Table 1). Based on these values we can compute a conservative minimum C_{27} sterol content of 88.1% for *Andiva* (Supplementary Text).
10

Using the remarkable steroid patterns of the fossils, it is possible to test the position of dickinsoniids on the phylogenetic tree. Lichen-forming fungi only produce ergosteroids, and even in those that host symbiotic algae, ergosteroids remain the major sterols (29, 30).
15 *Dickinsonia* contained no, or a maximum of only 0.23% ergosteroids, conclusively refuting the lichen hypothesis (7). The groups of rhizarian protists that include gigantic representatives (Gromiidae, Xenophyophorea and other Foraminifera), and their retarian relatives, all produce a complex mixture of sterols, with cholesteroloids comprising 10.3 to 78.2% of the mixture, ergosteroids 4.9 to 43.0% and stigmasteroids 7.2 to 60.1% (Table S4). Moreover, rhizarian protists may produce C_{30} sterols ($24n$ -propylcholestane) that can form a significant (up to around 20%) proportion of their total sterol content (31). By contrast, in most
20 *Dickinsonia* and *Andiva* extracts, C_{30} steroids were below detection limits. Thus, the steroid composition of dickinsoniids is markedly distinct from steroid distributions observed in Rhizaria, rendering a protozoan affinity of these fossils extremely unlikely. All animals, with rare exceptions such as some demosponges and bivalve molluscs, are characterised by
25 exclusive production of C_{27} sterols (32, 33). The closest relatives of metazoans, *Choanoflagellata* and *Filasterea*, produce 90–100% and 84–100% of cholesterol, respectively, and contain up to 16% ergosteroids (34–36). While the sterol composition of some choanoflagellates and filastereans falls within the range observed for *Dickinsonia* and *Andiva*,
30 they are unlikely precursor candidates since these groups are only ever represented by microscopic organisms, leaving a stem- or crown-group metazoan affinity as the only plausible phylogenetic position for *Dickinsonia* and its morphological relatives.

Molecular fossils firmly place dickinsoniids within the animal kingdom, establishing
35 *Dickinsonia* as the oldest confirmed macroscopic animals in the fossil record (558 Ma) next to marginally younger *Kimberella* from Zimnie Gory (555 Ma) (37). However alien they looked, the presence of large dickinsoniid animals, reaching 1.4 m in size (38), reveals that the appearance of the Ediacara biota in the fossil record is not an independent experiment in large body size but indeed a prelude to the Cambrian explosion of animal life.

40

References and Notes

1. R. C. Sprigg, Early Cambrian (?) jellyfishes from the Flinders Ranges, South Australia. *Transactions of the Royal Society of South Australia* **71**, 212-224 (1947).
2. M. F. Glaessner, *The dawn of animal life: a biohistorical study*. (Cambridge University Press, Cambridge, UK, 1984), pp. 244.
3. G. M. Narbonne, Modular Construction of Early Ediacaran Complex Life Forms. *Science* **305**, 1141-1144 (2004).
4. S. Xiao, M. Laflamme, On the eve of animal radiation: phylogeny, ecology and evolution of the Ediacara biota. *Trends Ecol Evol* **24**, 31-40 (2009).
5. M. Steiner, J. Reitner, Evidence of organic structures in Ediacara-type fossils and associated microbial mats. *Geology* **29**, 1119-1122 (2001).
6. K. J. Peterson, B. Waggoner, J. W. Hagadorn, A Fungal Analog for Newfoundland Ediacaran Fossils? *Integrative and Comparative Biology* **43**, 127-136 (2003).
7. G. J. Retallack, Ediacaran life on land. *Nature* **493**, 89-92 (2013).
8. A. Seilacher, The nature of vendobionts. *Geological Society, London, Special Publications* **286**, 387-397 (2007).
9. A. Y. Zhuravlev, Were Ediacaran Vendobionta multicellulars? *Neues Jahrbuch für Geologie und Paläontologie, Abhandlungen* **190**, 299-314 (1993).
10. G. M. Narbonne, THE EDIACARA BIOTA: Neoproterozoic Origin of Animals and Their Ecosystems. *Annual Review of Earth and Planetary Sciences* **33**, 421-442 (2005).
11. S. D. Evans, M. L. Droser, J. G. Gehling, Highly regulated growth and development of the Ediacara macrofossil Dickinsonia costata. *PLOS ONE* **12**, e0176874 (2017).
12. D. Grazhdankin, in *Encyclopedia of Geobiology*, J. Reitner, V. Thiel, Eds. (Springer Netherlands, Dordrecht, 2011), pp. 342-348.
13. D. H. Erwin *et al.*, The Cambrian Conundrum: Early Divergence and Later Ecological Success in the Early History of Animals. *Science* **334**, 1091-1097 (2011).
14. M. A. Fedonkin, B. M. Waggoner, The Late Precambrian fossil Kimberella is a mollusc-like bilaterian organism. *Nature* **388**, 868 (1997).
15. A. Y. Ivantsov, Trace fossils of precambrian metazoans “Vendobionta” and “Mollusks”. *Stratigraphy and Geological Correlation* **21**, 252-264 (2013).
16. J. B. Antcliffe, A. J. Gooday, M. D. Brasier, Testing the protozoan hypothesis for Ediacaran fossils: a developmental analysis of Palaeopascichnus. *Palaeontology* **54**, 1157-1175 (2011).
17. I. Bobrovskiy, J. M. Hope, A. Krasnova, A. Ivantsov, J. J. Brocks, Molecular fossils from organically preserved Ediacara biota reveal cyanobacterial origin for *Beltanelliformis*. *Nature Ecology & Evolution*, (2018).
18. S. Xiao *et al.*, Affirming life aquatic for the Ediacara biota in China and Australia. *Geology* **41**, 1095-1098 (2013).
19. M. L. Droser, J. G. Gehling, The advent of animals: The view from the Ediacaran. *Proceedings of the National Academy of Sciences* **112**, 4865-4870 (2015).
20. D. Grazhdankin, Patterns of Evolution of the Ediacaran Soft-Bodied Biota. *Journal of Paleontology* **88**, 269-283 (2014).
21. A. J. Gooday *et al.*, Giant protists (xenophyophores, Foraminifera) are exceptionally diverse in parts of the abyssal eastern Pacific licensed for polymetallic nodule exploration. *Biological Conservation* **207**, 106-116 (2017).
22. M. V. Matz, T. M. Frank, N. J. Marshall, E. A. Widder, S. Johnsen, Giant Deep-Sea Protist Produces Bilaterian-like Traces. *Current Biology* **18**, 1849-1854 (2008).

23. E. A. Sperling, J. Vinther, A placozoan affinity for Dickinsonia and the evolution of late Proterozoic metazoan feeding modes. *Evolution & Development* **12**, 201-209 (2010).
24. J. K. Volkman, Sterols and other triterpenoids: source specificity and evolution of biosynthetic pathways. *Organic Geochemistry* **36**, 139-159 (2005).
25. R. B. Kodner, A. Pearson, R. E. Summons, A. H. Knoll, Sterols in red and green algae: quantification, phylogeny, and relevance for the interpretation of geologic steranes. *Geobiology* **6**, 411-420 (2008).
26. T. M. Peakman, J. W. De Leeuw, W. I. C. Rijpstra, Identification and origin of $\Delta^8(14)5\alpha$ - and $\Delta^{14}5\alpha$ -sterenes and related hydrocarbons in an immature bitumen from the Monterey Formation, California. *Geochimica et Cosmochimica Acta* **56**, 1223-1230 (1992).
27. S. J. Gaskell, G. Eglinton, Sterols of a contemporary lacustrine sediment. *Geochimica et Cosmochimica Acta* **40**, 1221-1228 (1976).
28. I. D. Bull, M. J. Lockheart, M. M. Elhmmali, D. J. Roberts, R. P. Evershed, The origin of faeces by means of biomarker detection. *Environment international* **27**, 647-654 (2002).
29. J. D. Weete, M. Abril, M. Blackwell, Phylogenetic distribution of fungal sterols. *PLoS One* **5**, e10899 (2010).
30. S. Safe, L. M. Safe, W. S. G. Maass, Sterols of three lichen species: *Lobaria pulmonaria*, *Lobaria Scrobiculata* and *Usnea Longissima*. *Phytochemistry* **14**, 1821-1823 (1975).
31. J. Grabenstatter *et al.*, Identification of 24-n-propylidenecholesterol in a member of the Foraminifera. *Organic geochemistry* **63**, 145-151 (2013).
32. A. Kanazawa, Sterols in marine invertebrates. *Fisheries Science* **67**, 997-1007 (2001).
33. G. D. Love *et al.*, Fossil steroids record the appearance of Demospongiae during the Cryogenian period. *Nature* **457**, 718-721 (2009).
34. R. B. Kodner, R. E. Summons, A. Pearson, N. King, A. H. Knoll, Sterols in a unicellular relative of the metazoans. *Proc Natl Acad Sci U S A* **105**, 9897-9902 (2008).
35. D. A. Gold *et al.*, Sterol and genomic analyses validate the sponge biomarker hypothesis. *Proceedings of the National Academy of Sciences* **113**, 2684-2689 (2016).
36. S. R. Najle, M. C. Molina, I. Ruiz-Trillo, A. D. Uttaro, Sterol metabolism in the filasterean *Capsaspora owczarzaki* has features that resemble both fungi and animals. *Open Biology* **6**, (2016).
37. D. Graždankin, Patterns of distribution in the Ediacaran biotas: facies versus biogeography and evolution. *Paleobiology* **30**, 203-221 (2004).
38. R. Jenkins, Aspects of the geological setting and palaeobiology of the Ediacara assemblage. *Natural history of the flinders ranges* **7**, 33-45 (1996).
39. J. J. Brocks, E. Grosjean, G. A. Logan, Assessing biomarker syngeneity using branched alkanes with quaternary carbon (BAQCs) and other plastic contaminants. *Geochimica et Cosmochimica Acta* **72**, 871-888 (2008).
40. A. J. M. Jarrett, R. Schinteie, J. M. Hope, J. J. Brocks, Micro-ablation, a new technique to remove drilling fluids and other contaminants from fragmented and fissile rock material. *Organic Geochemistry* **61**, 57-65 (2013).
41. J. J. Brocks, J. M. Hope, Tailing of Chromatographic Peaks in GC-MS Caused by Interaction of Halogenated Solvents with the Ion Source. *Journal of Chromatographic Science* **52**, 471-475 (2014).
42. I. Björkhem, J.-Å. Gustafsson, Mechanism of Microbial Transformation of Cholesterol into Coprostanol. *European Journal of Biochemistry* **21**, 428-432 (1971).

43. F. Zollo, E. Finamore, D. Gargiulo, R. Riccio, L. Minale, Marine sterols. Coprostanols and 4 α -methyl sterols from mediterranean tunicates. *Comparative Biochemistry and Physiology Part B: Comparative Biochemistry* **85**, 559-560 (1986).
44. T. S. Milkova, S. S. Popov, N. L. Marekov, S. N. Andreev, Sterols from black sea invertebrates—I. Sterols from Scyphozoa and Anthozoa (Coelenterata). *Comparative Biochemistry and Physiology Part B: Comparative Biochemistry* **67**, 633-638 (1980).
45. S. B. Seidel, J. R. Proudfoot, C. Djerassi, D. Sica, G. Sodano, Minor and trace sterols from marine invertebrates 56. Novel coprostanols from the marine sponge petrosia ficiformis. *Steroids* **47**, 49-62 (1986).
46. R. C. Janaway, S. L. Percival, A. S. Wilson, in *Microbiology and Aging: Clinical Manifestations*, S. L. Percival, Ed. (Humana Press, Totowa, NJ, 2009), pp. 313-334.
47. H. Gill-King, Chemical and ultrastructural aspects of decomposition. *Forensic taphonomy: The postmortem fate of human remains*, 93-108 (1997).
48. A. Y. Ivantsov, Feeding traces of proarticulata—the Vendian metazoa. *Paleontological Journal* **45**, 237-248 (2011).
49. J. N. Ricci, R. Morton, G. Kulkarni, M. L. Summers, D. K. Newman, Hopanoids play a role in stress tolerance and nutrient storage in the cyanobacterium *Nostoc punctiforme*. *Geobiology*, n/a-n/a (2016).
50. R. E. Summons, L. L. Jahnke, J. M. Hope, G. A. Logan, 2-Methylhopanoids as biomarkers for cyanobacterial oxygenic photosynthesis. *Nature* **400**, 554-557 (1999).
51. P. V. Welander, M. L. Coleman, A. L. Sessions, R. E. Summons, D. K. Newman, Identification of a methylase required for 2-methylhopanoid production and implications for the interpretation of sedimentary hopanes. *Proceedings of the National Academy of Sciences* **107**, 8537-8542 (2010).
52. M. Rohmer, P. Bouvier-Nave, G. Ourisson, Distribution of Hopanoid Triterpenes in Prokaryotes. *Microbiology* **130**, 1137-1150 (1984).
53. J. N. Ricci *et al.*, Diverse capacity for 2-methylhopanoid production correlates with a specific ecological niche. *ISME J* **8**, 675-684 (2014).
54. K. Peters, C. Walters, J. Moldowan, *The Biomarker Guide. Volume 2. Biomarkers and Isotopes in Petroleum Systems and Earth History*. (Cambridge University Press, New York, ed. 2nd, 2005), pp. 634.
55. Y. V. Kissin, Catagenesis and composition of petroleum: Origin of n-alkanes and isoalkanes in petroleum crudes. *Geochimica et Cosmochimica Acta* **51**, 2445-2457 (1987).

35

Acknowledgments: We thank E. Luzhnaya, A. Krasnova, A. Nagovitsyn, P. Rychkov, V. Rychkov and S. Rychkov for their help with collecting Ediacaran fossils, E. Golubkova with organizing one of the field trips, P. Pringle and R. Tarozo for laboratory support, F. Not, C. Schmidt, R. Schiebel, P. De Deckker, S. Eggins, J. Pawlowski, S. S. Bowser and M. Stuhr for rhizarian specimens; **Funding:** The study is funded by Australian Research Council grants DP160100607 and DP170100556 (to J.J.B.), Russian Foundation for Basic Research project No. 17-05-02212A (A.I. and I.B) and the Max-Planck-Society (C.H.). I.B. gratefully acknowledges an Australian Government Research Training Program stipend scholarship, and B.J.N. a Geobiology fellowship of the Agouon Institute. **Author contributions:** I.B. designed the study and analysed biomarkers from Ediacaran fossils, J.M.H. helped with biomarker analysis, I.B. and A.I. collected fossils, B.J.N., C.H., J.M.H. and J.J.B. analysed modern Rhizaria, I.B. and J.J.B. interpreted data and wrote the manuscript with contributions

from all authors; **Competing interests:** Authors declare no competing interests; **Data and materials availability:** All data required to understand and assess the conclusions of this research are available in the main text and supplementary materials.

Supplementary Materials:

5 Materials and Methods

Supplementary Text

Figs. S1 to S6

Tables S1 to S4

References (39-55)

10

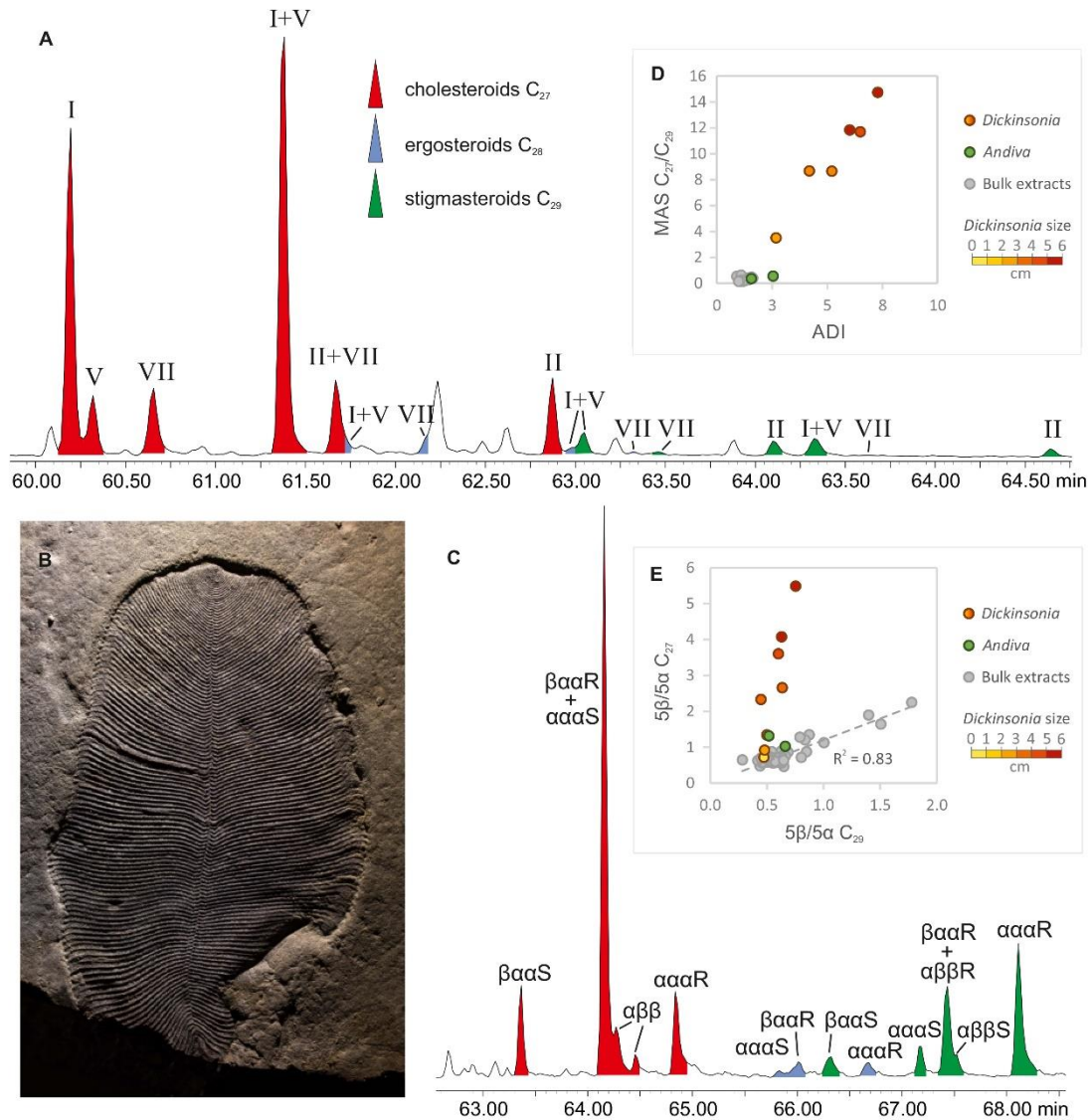


Fig. 1. Biomarkers from organically preserved *Dickinsonia*. (A) m/z 253 selected ion recording (SIR) chromatogram showing the distribution of monoaromatic steroids (MAS) of the solvent extract of a large *Dickinsonia* specimen (*Dickinsonia*-2; 5.5 cm width); (B) organically preserved *Dickinsonia* from the Lyamtsa locality (*Dickinsonia*-2); (C) metastable reaction monitoring (MRM) chromatogram showing the sum of C_{27-29} sterane traces of *Dickinsonia*-2; $\alpha\beta\beta = 5\alpha(H), 14\beta(H), 17\beta(H)$ (and correspondingly for $\alpha\alpha\alpha$ and $\beta\alpha\alpha$), S and R indicates isomerisation at position C-20; (D) relationship between the MAS $C_{27}/MAS C_{29}$ ratio and the Animal Decomposition Index $ADI = (C_{27} 5\beta/5\alpha)/(C_{29} 5\beta/5\alpha)$ in *Dickinsonia* ($n = 6$), *Andiva* ($n = 2$) and bulk rock extracts from the Lyamtsa and Zimmie Gory localities ($n = 32$); only samples with detectable MAS were used in the plot; ADI is a measure of the quantity of sterols that decomposed in the anaerobic microenvironment of an animal carcass relative to normal sterol decomposition within the background sediment. $ADI \approx 1$ indicates that cholesteroids and stigmasteroids underwent alteration in the same diagenetic environment consistent with the absence of animal tissue. $ADI > 1$ indicates contribution of animal steroids to the biomarker signal. (E) Relationship between the $5\beta/5\alpha$ sterane isomer ratio for cholestane (C_{27}) and stigmastane (C_{29}) in *Dickinsonia* ($n = 8$), *Andiva* ($n = 2$) and bulk rock extracts from the Lyamtsa and Zimmie Gory localities ($n = 54$); $5\beta/5\alpha = (\beta\alpha\alpha$

20R+ $\alpha\alpha\alpha$ 20S)/ $\alpha\alpha\alpha$ 20R. MAS structures: I = 5 β (H)10 β (CH₃), II = 5 α (H)10 β (CH₃), V = 5 β (CH₃)10 β (H), VII = 5 α (CH₃)10 α (H).

Sample	Locality	Size (width, cm)	Saturated steranes								Monoaromatic steroids ⁴			
			C ₂₇ %	C ₂₈ %	C ₂₉ %	C ₃₀ % ¹	C ₂₇ 5 β /5 α ²	C ₂₈ 5 β /5 α ²	C ₂₉ 5 β /5 α ²	ADI ³	C ₂₇ %	C ₂₈ %	C ₂₉ %	C ₂₇ /C ₂₉
<i>Dickinsonia-1</i>	Lyamtsa	6.0	48.1 (1.3) ⁵	5.7 (0.2)	45.8 (1.2)	0.4 (0.04)	3.61 (0.21)	0.52 (0.34)	0.60 (0.06)	6.01 (0.67)	92.4 (2.5)	2.1 (0.1)	5.5 (0.3)	11.84 (0.93)
<i>Dickinsonia-2</i>	Lyamtsa	5.5	63.2 (1.5)	4.9 (0.2)	31.9 (0.8)	0 {0.05} ⁶	5.49 (0.28)	0.65 (0.34)	0.75 (0.06)	7.28 (0.65)	93.0 (2.3)	1.8 (0.1)	5.2 (0.3)	14.75 (0.91)
<i>Dickinsonia-3</i>	Lyamtsa	4.5	47.9 (1.5)	6.1 (0.3)	46.0 (1.4)	0 {0.03}	4.08 (0.29)	0.75 (0.34)	0.63 (0.04)	6.50 (0.64)	92.5 (3.2)	2.7 (0.2)	4.8 (0.3)	11.71 (1.41)
<i>Dickinsonia-4</i>	Lyamtsa	4.0	33.4 (2.2)	8.0 (0.7)	58.5 (3.5)	0 {0.08}	2.66 (0.41)	0.97 (0.34)	0.64 (0.08)	4.18 (0.83)	87.9 (6.4)	4.8 (0.7)	7.3 (0.9)	8.67 (1.59)
<i>Dickinsonia-5</i>	Lyamtsa	4.0	44.8 (0.9)	7.6 (0.4)	47.6 (1.0)	0 {0.01}	2.33 (0.10)	0.81 (0.34)	0.45 (0.02)	5.21 (0.32)	91.3 (4.5)	3.6 (0.4)	5.1 (0.5)	8.66 (1.81)
<i>Dickinsonia-6</i>	Lyamtsa	3.5	27.5 (0.7)	9.9 (0.5)	62.6 (1.3)	0 {0.04}	1.34 (0.07)	0.79 (0.34)	0.50 (0.02)	2.67 (0.18)	84.8 (5.7)	3.4 (0.5)	11.8 (1.2)	3.51 (0.80)
<i>Dickinsonia-7</i>	Lyamtsa	1.0	17.2 (1.2)	6.9 (1.2)	75.9 (3.6)	0 {0.18}	0.71 (0.10)	0.22 (0.34)	0.47 (0.05)	1.49 (0.26)	-	-	-	-
<i>Dickinsonia-8</i>	Lyamtsa	2.5	20.5 (1.3)	6.7 (1.2)	72.7 (3.6)	0 {0.10}	0.91 (0.13)	0.26 (0.34)	0.48 (0.05)	1.89 (0.32)	-	-	-	-
<i>Dickinsonia-Sandstone</i>	Lyamtsa	-	11.6 (0.3)	8.9 (0.2)	78.9 (1.2)	0.6 (0.04)	0.64 (0.04)	0.85 (0.34)	0.52 (0.02)	1.23 (0.08)	11.9 (1.0)	16.8 (1.5)	71.3 (4.4)	0.17 (0.01)
<i>Dickinsonia-Clay</i>	Lyamtsa	-	9.7 (0.3)	7.8 (0.2)	82.0 (1.3)	0.5 (0.03)	0.61 (0.03)	0.71 (0.34)	0.59 (0.02)	1.03 (0.07)	10.6 (0.7)	13.4 (0.9)	76.0 (3.3)	0.2 (0.01)
<i>Andiva-1</i>	Zimnie Gory	8.0	24 (0.4)	10.3 (0.3)	64.3 (0.9)	1.3 (0.1)	1.07 (0.04)	0.76 (0.34)	0.68 (0.02)	1.55 (0.07)	21.5 (0.8)	17.5 (0.7)	61.0 (1.9)	0.36 (0.01)
<i>Andiva-2</i>	Zimnie Gory	4.0	24.9 (1.2)	12.2 (1.2)	61.8 (2.7)	1.0 (0.2)	1.31 (0.15)	0.81 (0.34)	0.52 (0.04)	2.54 (0.36)	29.3 (2.6)	12.6 (1.4)	58.1 (4.5)	0.55 (0.05)
<i>Andiva Mat</i>	Zimnie Gory	-	25.8 (1.0)	15.8 (1.0)	57.4 (1.9)	1.0 (0.1)	0.80 (0.07)	0.96 (0.34)	0.65 (0.04)	1.24 (0.13)	18.7 (1.4)	21.4 (1.6)	59.8 (3.5)	0.35 (0.02)
<i>Andiva-Sandstone</i>	Zimnie Gory	-	37.5 (1.0)	10.5 (0.3)	51.6 (1.3)	0.5 (0.04)	0.65 (0.04)	0.91 (0.34)	0.61 (0.03)	1.08 (0.08)	25.6 (1.7)	15.7 (1.2)	58.7 (3.4)	0.43 (0.03)
<i>Andiva-Clay</i>	Zimnie Gory	-	23.1 (0.5)	9.5 (0.3)	65.9 (1.3)	1.5 (0.02)	0.86 (0.04)	0.84 (0.34)	0.68 (0.02)	1.26 (0.07)	19.4 (1.6)	11.2 (1.2)	69.4 (4.7)	0.28 (0.02)

5

Table 1. Steroid distributions in *Dickinsonia* and *Andiva* extracts.

¹C₃₀ steranes are only represented by 24-isopropylcholestanes; ²5 β /5 α = ($\beta\alpha\alpha$ 20R+ $\alpha\alpha\alpha$ 20S)/ $\alpha\alpha\alpha$ 20R; ³Animal Decomposition Index ADI = (C₂₇ 5 β /5 α)/(C₂₉ 5 β /5 α) (see Figure 1 caption); ⁴only the I and V monoaromatic steroid isomers (see Figure 1 for nomenclature) were used for all computations as they display the least coelution with other peaks on the chromatogram; ⁵numbers in parentheses are standard deviation values; ⁶numbers in braces ‘{ }’ next to zero values represents the detection limit, i.e. the maximum of a given compound that may be present when not detected.

10

Supplementary Materials for

5

Ancient steroids establish the Ediacaran fossil *Dickinsonia* as one of the earliest animals

10

Ilya Bobrovskiy*, Janet M. Hope, Andrey Ivantsov, Benjamin J. Nettersheim, Christian Hallman, Jochen J. Brocks*

*Correspondence to: ilya.bobrovskiy@anu.edu.au, jochen.brocks@anu.edu.au

15 **This PDF file includes:**

Materials and Methods
Supplementary Text
Figs. S1 to S6
20 Tables S1 to S4

Materials and Methods

Sample collection

5 Biomarker analyses were conducted on organically preserved macrofossils *Dickinsonia*
and *Andiva* (Fig. 1; Fig. S1), microbial mats surrounding the fossils, and bulk extracts of
sedimentary rocks enclosing the fossils. Samples were collected during fieldwork in the
Lyamtsa and Zimnie Gory localities of the Ediacara Biota in the White Sea Region (Russia) in
2015–2017 specifically for biomarker analysis. *Dickinsonia* (8 specimens) come from a surface
10 in the lower part of the Lyamtsa Beds (Ust-Pinega Formation, Redkino Regional Stage),
exposed to the south of Lyamtsa Village. The fossils were underlain by clay with mm-thick
lenses of siltstone and sandstone, and buried under 30 cm-thick sandstone layer, composed of
thinner (5-10 cm) beds with hummocky cross-stratification, separated by microbially induced
15 wrinkle structures. *Andiva* (2 specimens) were collected from a surface in the lower part of the
Erga Beds (Mezen Formation, Kotlin Regional Stage). The fossils were also underlain by clay
with mm-thick lenses of siltstone and sandstone and covered with 40-60 cm thick lenses of
massive sandstone with soft sediment deformations and thick (up to 5 cm thick) load cracks at
the bottom. Samples used for determining the background signal ($n=54$) were collected from
20 Lyamtsa and Verkhovka Beds (Ust-Pinega Formation, Redkino Regional Stage) of the
Lyamtsa locality and from Vaysitsa, Zimnie Gory (Ust-Pinega Formation, Redkino Regional
Stage) and Erga Beds (Mezen Formation, Kotlin Regional Stage) of the Zimnie Gory locality.
All samples were collected avoiding weathered zones and cracks and were immediately
wrapped in pre-combusted aluminium foil (300°C, 9h) and packed in calico cotton bags under
strict avoidance of contamination (17).

25 Sterol signatures of rhizarian protists were determined on natural specimens. *Sorites* sp.
and *Amphistegina lobifera* were collected attached to pebbles by snorkelling in shallow water
1-3 m in Eilat, Israel and subsequently kept under controlled laboratory conditions for four
months until they were handpicked again and cleaned with a brush prior to laboratory analyses.
The two Foraminifera *Shepherdella* sp. (collected at the Gulf of Eilat) and *Quinqueloculina*
30 sp. (collected at the Mediterranean coast of Tel Aviv, Israel) were extracted shortly after
collection in the field after separation and cleaning with tweezers and brushes. Brightly orange
Shepherdella sp. allogromid Foraminifera were picked from rocks and sea-grass. Collodarian
radiolarians were handpicked from the contents of a plankton net collected from surface waters
in the Villefranche sur Mer bay (France). *Gromia* sp. were collected by Scuba Divers from the
bottom sediments at the McMurdo Station jetty in Antarctica and pickled in ethanol. A bulk
35 *Acantharea* sample was collected using a plankton tow net during a bloom event of *Acantharea*
sp. in the shallow Twofold Bay near Eden, SE Australia that is open to the Tasman Sea. After
collection, the sample was washed with freshwater and pickled in 100% ethanol, then kept
frozen until analysis at the Australian National University.

40 Fossils characteristics

The thickness of organic matter of *Dickinsonia* was estimated based on a thin section
made through one of the fossil specimens. The size of fossil specimens was determined based
on their width as most of the analysed specimens were not complete and lacked either of their

ends. These size measurements are estimates as all dickinsoniids were deformed before or during burial.

Sample preparation and extraction

5 Organic matter of the fossils was separated from the sandstone surface using 5% hydrochloric acid (several drops on the surface of a fossil) and 30% hydrofluoric acid (several drops on the surface of a fossil, followed by drying, repeated two times). Fossils were then placed into a glass beaker filled with water to remove acid, allowing most of organic matter to detach from remaining inorganic components of the fossils. Any remaining organic matter
10 attached to the rock was separated with a scalpel. Combined organic matter was neutralized in deionized (Millipore Elix 3UV, France) water under ultrasonic agitation and subsequently centrifuged (3 times) to remove remaining acids. Hydrocarbons were extracted from the organic matter via ultrasonic agitation in solvents (methanol for 30 min, dichloromethane (DCM) for 15 min (x 2), DCM : *n*-hexane 1 : 1 for 15 min). All solvents were 99.9% grade (UltimAR®; Mallinckrodt Chemicals, St. Louis, MO, USA). Glassware was cleaned by
15 combustion at 300°C for 9 h.

Bulk sedimentary samples (represented by clay, heterolithic interlamination and sandstones) were analysed using the so-called Exterior-Interior protocol described in detail elsewhere (17, 39, 40). Briefly, exterior ('E') 3–4 mm of rock samples were removed using a
20 micro drill (Dremel® 400 Series Digital, Mexico) with a solvent cleaned saw nozzle. Analysis of the last saw-blade solvent rinse confirmed that it was free of detectable contaminants. The exterior and the interior portions of each sample were ground to powder (>240 mesh) using a steel puck mill (Rocklabs Ltd., Onehunga, New Zealand). The mill was cleaned using methanol and dichloromethane, and by grinding combusted (600°C, 9 h) quartz sand.

25 Bitumen was extracted from rock powder using an Accelerated Solvent Extractor (ASE 200, Dionex, USA) with DCM : methanol (9:1), reduced to 100 µL under a stream of nitrogen gas, and then fractionated into saturated, aromatic and polar fractions using micro-column chromatography over annealed (300°C; 12 h) and dry packed silica gel (Silica Gel 60; 230–600 mesh; EM Science). Saturated hydrocarbons were eluted with 1 dead volume (DV) of *n*-hexane, aromatic hydrocarbons with 4.5 DV of *n*-hexane : DCM (1 : 1) and the polar fraction
30 with 3 ml DCM : methanol (1 : 1). Extracts from fossils with low hydrocarbon content were only fractionated into saturated+aromatic and polar fractions to reduce the probability of contamination and loss of analytes. An internal standard, 18-MEAME (18-methyleicosanoic acid methylester; Chiron Laboratories AS), was added to the saturated and aromatic fractions,
35 while D4 (*d*₄-C₂₉-αααR-ethylcholestane; Chiron Laboratories AS) was added to saturated and saturated+aromatic hydrocarbon fractions with low biomarker content. The samples were analysed and quantified by GC–MS.

Biomass of rhizarian protists (Extended Data Table 4) was extracted thrice using a modified Bligh and Dyer method (DCM:MeOH:H₂O=1:2:0.4, then 2:2:0.4, then 2:2:1.4) or by
40 ultrasonic agitation in DCM : MeOH (9 : 1). *Gromia* specimens were stored in ethanol after sampling and the ethanol was analysed in the same manner as the other extracts. The total lipid extracts were separated into hydrocarbons (F1), esters and ketones (F2), alcohols (F3) and fatty acids (F4) by small-scale open column chromatography over aminopropyl-substituted silica gel (Chromabond Sorbent NH₂, Macherey-Nagel, Germany; 500 mg in a 6 mL glass SPE column), where F1 was eluted with 4 mL *n*-hexane, F2 with 6 mL *n*-hexane:DCM (3:1), F3
45

with 7 mL DCM:acetone (9:1) and F4 with 8 mL DCM containing 2% formic acid. F3 was hydrogenated by bubbling a gentle stream of hydrogen gas into a 4 mL vial filled with *n*-hexane, F3 lipids and platinum (IV) oxide (ca. 7 mg) under stirring for >4h. Converted steranes were purified by eluting with an excess of *n*-hexane over a small chromatographic column filled with activated silica gel. Blank hydrogenations were run before and after samples to assess contamination. *Acantharea* sp. lipids were extracted with a similar modified Bligh and Dyer method, and saponified with 5 % KOH in MeOH : H₂O (8 : 2) and neutral lipids were recovered by addition of H₂O and the same amount of Hex : DCM (4:1), pyrolysed at 320 °C for 21 h in an evacuated glass tube and hydrogenated with PtO₂ overnight.

10

Gas chromatography–mass spectrometry (GC-MS)

GC-MS analyses of Ediacaran and *Acantharea* extracts were carried out on an Agilent 6890 gas chromatograph coupled to a Micromass Autospec Premier double sector mass spectrometer (Waters Corporation, Milford, MA, USA) at the Australian National University. The GC was equipped with a 60 m DB-5 MS capillary column (0.25 mm i.d., 0.25 µm film thickness; Agilent JW Scientific, Agilent Technologies, Santa Clara, CA, USA), and helium was used as the carrier gas at a constant flow of 1 mL min⁻¹. Samples were injected in splitless mode into a Gerstel PTV injector at 60°C (held for 0.1 min) and heated at 260°C min⁻¹ to 300°C. For full-scan, selected ion recording (SIR) and metastable reaction monitoring (MRM) analyses, the GC oven was programmed from 60°C (held for 4 min) to 315°C at 4°C min⁻¹, with total run time of 100 min. All samples were injected in *n*-hexane to avoid deterioration of chromatographic signals by FeCl₂ build-up in the MS ion source through use of halogenated solvents (41). *n*-Alkanes were quantified in full-scan mode in *m/z* 85 trace, and $\alpha\alpha\alpha$ 20R-stigmastane – in *m/z* 217 trace, relative to the 18-MEAME internal standard (*m/z* 340). Steranes and hopanes were quantified in MRM mode in M⁺ → 217 and M⁺ → 191 transitions respectively relative to $\alpha\alpha\alpha$ 20R-stigmastane. Monoaromatic steroids were quantified in SIR mode using the *m/z* 253 base ion. Peak areas are uncorrected for differences in GC-MS response.

Hydrogenated rhizarian steroids were analysed on a Thermo Quantum XLS Ultra triple quadrupole MS coupled to a Thermo Trace GC at the University of Bremen. The GC was fitted with a VF-1 ms (40m; 0.15 µm; 0.15 mm), DB-XLB (60 m; 0.25 mm; 0.25 µm) or DB-35 ms (60 m; 0.25 mm; 0.25 µm) capillary column and operated under a constant flow (1.3 mL/min.) of helium (99.999% pure, Westfalen AG). Samples were injected in splitless mode using a Thermo PTV injector, while the oven was ramped from 60°C (5 mins. isothermal) to 325°C at 4°/min. and held at final temperature for 25 mins. Electron impact ionization was achieved at 70 eV and 250°C with an emission current of 50 mA. The MS was operated in 0.7 Da resolution (Q1 and Q3) with a cycle time of 0.5 sec, while Q2 was operated with Argon (99.999% pure; Westfalen AG) at a pressure of 1.1 mtorr and varying collision voltages. Analytes were identified in comparison to the NSO-1 oil standard and quantified on characteristic parent-to-daughter ion mass transitions (*m/z* 372, 386, 400 and 414 fragmenting to 217) without correcting for differences in response. Ediacaran biomarker peaks were identified based on relative retention time in comparison with AGSO industrial standard (a standard mixture of oils of different ages) and literature data. Identification of $\beta\alpha\alpha$ sterane isomers was additionally confirmed by mass spectra obtained in full-scan mode.

45

Error quantification

As repeat injections of fossil extracts were not possible due to the limited abundance of valuable sample material, standard deviations for the concentration of each biomarker were externally determined using the AGSO industrial standard. The main sources of quantification error in extracts are low signal to noise ratios of molecular peaks in mass chromatograms. We explored the relationships between signal/noise ratio and coefficient of variation for our specific GC-MS system for each quantified compound using five repeat injections of the AGSO Standard. MRM signal areas of steranes, hopanes, cheilanthanes and the D4 internal standard were integrated for each repeat run and plotted against the coefficient of variation C_v for the five repeats (Fig. S3; C_v was computed for the ratio of compound signal relative to the highest biomarker peak, $C_{30} 17\alpha(H)21\beta(H)$ hopane). The plot yields a relationship described by the formula $C_v = 186.18x^{-0.31}$ ($R^2 = 0.82$), where x is the integrated peak area. The standard deviation for each GC-MS signal in sample extracts used in this study was calculated based on this relationship ($STD = C_v * \text{signal area}$). For biomarker ratios, error propagation followed standard root mean square error propagation formulae. As an estimate of the maximum content of compounds that were below detection limits, the smallest visible peak in corresponding chromatograms was integrated.

As $\beta\alpha\alpha$ 20R-ergostane (5β) coelutes with two other compounds, $\alpha\alpha\alpha$ 20S-ergostane and an unknown sterane (tentatively identified as a $\beta\alpha\alpha$ 20R-27-nor-sterane), its integration error should be expected to be much higher than the error for peaks that are not coeluting and are mainly controlled by signal/noise ratio. Therefore, we estimated an error by comparing measured and computed values for 5β 20R-ergostane. In bulk extracts, $5\beta/5\alpha$ ratios should theoretically be identical for all three sterane pseudohomologues, i.e. for cholestanes, ergostanes and stigmastanes (26). We thus measured the $5\beta/5\alpha$ ratios of cholestanes and stigmastanes in bulk sediment extracts (Fig. 1E) and used the average of $5\beta/5\alpha$ of cholestanes and stigmastanes in each individual sample to predict a theoretical $5\beta/5\alpha$ value for ergostanes. The average deviation of calculated and measured values across 54 samples was used as the standard deviation for this ratio.

30 Laboratory system blanks

A comprehensive, accumulatory system blank was performed covering all analytical steps from rock surface removal, extraction, fractionation to instrumental analysis. For this purpose, combusted (600°C, 9 h) sand was used to monitor background contamination during grinding, extraction, and fractionation processes.

Supplementary Text

Biomarker composition of dickinsoniids

5 β /5 α sterane isomers ratio

5 The elevated 5 β /5 α ratio of cholestane (up to 5.5) detected in all dickinsoniid fossils (Table 1, Figs. 1C,D,E) is rarely observed in nature and the geological record. Yet more unusual, in the dickinsoniids only cholestane 5 β /5 α is elevated while the corresponding ergostane and stigmastane ratios show the typical sedimentary background value 5 β /5 α \approx 0.6. Such a discrepancy between sterane pseudohomologues has, to our knowledge, never been
10 observed before in the fossil record. Under usual sedimentary conditions, the 5 β isomer is generated by hydrogenation of Δ^5 sterenes (sterenes with a double bond in position 5 of the ring system), while 5 α is formed from Δ^4 sterenes. The biological configuration of most biological sterols is Δ^5 . However, due to double bond isomerisation between the Δ^5 and Δ^4 positions, the equilibrium ratio between the 5 β and 5 α sterane isomers in an abiological
15 thermodynamically driven system is $\Delta^5 \rightarrow 5\beta : \Delta^4 \rightarrow 5\alpha = 39:61$, resulting in 5 β /5 α = 0.64 (26). This proportion is characteristic of bulk rock extracts from the White Sea Area (average 5 β /5 α = 0.64 \pm 0.26, n = 54), but is much lower than 5 β /5 α cholestane ratios in all dickinsoniid fossils. An origin of such elevated 5 β /5 α sterane ratios as observed in *Dickinsonia* can be explained by
20 microbial or dietary hydrogenation of unsaturated sterols to 5 β -stanols, common under strictly anaerobic conditions, and their further dehydration to Δ^3 5 β -sterenes and subsequent reduction to 5 β -steranes (26, 27, 42). These processes, when occurring within sediment, affect all steroid pseudohomologs equally, regardless of side chain methylation (26). In order to create the elevated 5 β /5 α cholestane ratio observed in the dickinsoniid extracts, only C₂₇ sterols could
25 have been subject to this mode of decay in a strongly anaerobic microenvironment. Sterols from the surroundings of the fossils were degraded under different taphonomic conditions, allowing us to discern the signal of fossils and background.

In principle, the elevated 5 β /5 α cholestane ratios and the strong aromatization of cholesteroids (Table 1) in dickinsoniids may arise from the presence of an unusual C₂₇ steroid, e.g. possessing multiple unsaturations. Additionally, the gut microbiota of some mammals,
30 including humans, transforms cholesterol to coprostanol (5 β -cholestanol) (28), resulting in the formation of 5 β -steranes during diagenesis. Thus, it is tempting to speculate that dickinsoniids possessed a gut or other digestive systems, and also microbiota responsible for this process. However, elevated 5 β /5 α ratios were also detected for C₂₇ to C₂₉ steranes in some sediment
35 extracts (5 β /5 α = up to 2.3; Fig. 1E) and in Ediacaran macroalgae from the White Sea with 5 β /5 α as high as 3.7 for cholestane, ergostane and stigmastane (Fig. S4) (17). The data show that elevated 5 β /5 α ratios form in sedimentary environments during decomposition of organic matter, and that these processes are not restricted to Ediacaran microfossils.

The elevated 5 β /5 α cholestane ratio in dickinsoniid fossil extracts is consistent with an origin from decomposing animal tissues. The occurrence of 5 β -stanols has been recorded even
40 in freshly collected marine animals on initial stages of decomposition (43, 44). In such cases, formation of 5 β -stanols can be connected with microbial transformation of animal tissue, independent of the structure of the precursor sterol. For instance, in decaying sponges, unusual sponge sterols were also found to be affected by this process, resulting in formation of 5 β -dihydro stanols (45). Anaerobic degradation of lipids via hydrogenation also dominates in
45 human remains, which is well studied in forensic taphonomy (46, 47).

Determination of exact sterol composition of Dickinsonia

Dickinsoniids inhabited a sea floor covered by microbial mats (Fig. 1B, Figs. S1,S2). Such microbial mats presumably developed over weeks, months or even years, accumulating senescent biomass of mat inhabitants and plankton. After burial by mud or sand, the organic matter of mats, plankton and dickinsoniids fused (Figs. S2A,B,C), making it impossible to physically separate the biomass. Thus, to determine the molecular composition of dickinsoniids, the molecular signal from the underlying mat needs to be separately determined and subtracted.

The determination of the background signal coming from the mat is a technical challenge. Measurement of the molecular signal of the mat directly surrounding the fossils (e.g. Fig. S1A) yielded extracts with extremely low signal/noise ratios (Table 1) and thus intolerably high propagated errors, or did not yield any detectable biomarkers. Moreover, it was unclear whether decaying and liquefied biomass from dickinsoniids would spill along the bedding plane, creating a halo around the carcass and affecting the taphonomy of molecules that do not belong to the organism. Furthermore, dickinsoniid fossils may contain dietary organic matter ('gut content', if dickinsoniids had a gut (48)), and this organic matter would be transformed in similar microenvironments as indigenous dickinsoniid tissue, complicating the signal further.

Variations in steroid composition of the extracts of different *Dickinsonia* specimens can be described by a two-component mixing system curve as a result of mixing between the steroids of the background signal and steroids directly derived from *Dickinsonia* (Fig. S2D). The mixing scenario is generally described by $x = n*x_1 + (1-n)*x_2$ where x is the concentration of a compound in the mixture, and x_1 and x_2 are the concentrations of that compound in the two components. In Figure S2D, the steroid composition for the background was taken as the average of sediment directly under- and overlying *Dickinsonia* (Table 1), and the concentrations of steranes and MAS in *Dickinsonia* were adjusted to best describe the data. The resulting relationship between sterane C₂₇ (%) and MAS C₂₇ (%) allows to estimate that *Dickinsonia* largely or exclusively produced C₂₇ sterol (~95–100%) and that aromatisation of sterols during the decay of *Dickinsonia* was more pronounced than in the background (Fig. S2D). The extrapolation, however, is not precise enough to discern whether living *Dickinsonia* contained small quantities of indigenous C₂₈ and C₂₉ sterols.

We were able to obtain a more precise sterol composition of *Dickinsonia* by quantifying bacterial hopanes in several *Dickinsonia* specimens. Hopanes are largely derived from aerobic bacteria; they are extremely uncommon in anaerobes (49). As *Dickinsonia* was degraded under largely anaerobic conditions (see above), the hopanes in the fossil extracts must be largely derived from the underlying mat or the surrounding sediment. Thus, the hopane content in individual *Dickinsonia* extracts is a measure for the magnitude of the background signal. To subtract the background and to estimate the relative proportion of cholesteroloids, ergosteroids and stigmasteroids of living *Dickinsonia* we used the three largest specimens with the best signal/noise ratios (Table 1). First we quantified the variance of the three eukaryotic monoaromatic steroids relative to hopanes between the *Dickinsonia* extracts (Table S1). The steroid/hopane ratio of steroids that are solely derived from the background should stay constant, while the ratio for steroids produced by *Dickinsonia* as well as the background should vary with a varying *Dickinsonia*/background biomass ratio. To determine this mathematically, for each of the MAS/H ratios we used a standard MS Office Excel variance VAR.S formula

$VAR.S = \sum(x - \bar{x})^2 / (n - 1)$, where x is a MAS/H value for each MAS homolog in an extract, \bar{x} is a mean value between the extracts and n is the number of samples ($n = 3$).

5 The ratios of ergosteroids and stigmasteroids over hopanes remained nearly constant across the three fossil extracts with very small variances ($0.076 \cdot 10^{-4}$ for ergosteroids and $0.024 \cdot 10^{-4}$ for stigmasteroids; Table S1). By contrast, the content of cholesteroloids relative to hopanes changed with a three order of magnitude higher variance ($33 \cdot 10^{-4}$). These data indicate that the bulk of cholesteroloids must come from the dickinsoniids while almost all of the ergosteroids and stigmasteroids, together with the bacterial hopanes, represent a constant background signal, presumably coming from the underlying microbial mat containing biomass
10 of bacteria and algae. Based on the computed variances, the proportion of each steroid variability can be estimated in % relative to the total variability (sum of all three steroid/hopane ratios). Such quantification of *Dickinsonia* steroid composition is based on the assumption that the background has no variability in steroid homolog proportions or relative hopane abundances. This is a conservative assumption because if the steroid/hopane ratios of the
15 background were not constant, then ergosteroid and stigmasteroid variability would increase and their estimated content in dickinsoniids would go up. Based on these assumptions, we compute a minimum cholesteroloid content of *Dickinsonia* of 99.7%, while the maximum ergosteroid content is 0.23% and stigmateroids 0.07% (Table S1).

20 Similar computations can be made based on variability of $5\beta/5\alpha$ sterane ratios in *Dickinsonia* extracts. Unfortunately, an assumption that the background signal is invariable, necessary for this computation, does not fully apply to $5\beta/5\alpha$ sterane background ratios (an average $5\beta/5\alpha$ value between all background signals is 0.65, ranging however from 0.28 to 1.78, $n = 54$; Fig. 1C). In our computations, this variability in the background signal, which is likely due to natural variations in diagenesis (see above), would artificially elevate the
25 ergosteroid and stigmasteroid proportion of *Dickinsonia*. However, even based on this imperfect data, the computation yields a conservative minimum C_{27} steroid content for *Dickinsonia* of 98.4%, while the maximum proportions of ergosteroids and stigmasteroids are 1.1% and 0.54% respectively (Table S1).

30 *Estimation of the sterol composition of Andiva*

Andiva specimens for this study were exclusively recovered from the Zimmie Gory locality. At Zimmie Gory, the proportion of sedimentary background signal in fossil extracts was far higher than at the Lyamtsa locality, where *Dickinsonia* was recovered. Thus, for *Andiva* it is more difficult to separate the dickinsoniid signal from the background. Moreover, the
35 methodology employed for *Dickinsonia*, i.e. computation of the variance of MAS/hopane ratios, was not possible for *Andiva* because the background MAS signal is too high. However, a rough estimate of the sterol composition of *Andiva* was possible based on $5\beta/5\alpha$ sterane ratios the same way as for *Dickinsonia*, but in this case using variability in $5\beta/5\alpha$ ratios for each sterane between the analysed *Andiva* extracts and an extract of surrounding microbial mat.
40 With the assumptions discussed above, the most conservative estimate for the minimum C_{27} steroid content of *Andiva* is 88.1%, while the maximum proportions of ergosteroids and stigmasteroids are 1.2% and 10.7% respectively (Table S2).

Other biomarkers

Hopanes

All extracts exhibit typical immature hopane distributions with low $T_s/(T_s+T_m)$ and $S/(S+R)$ ratios, high $\beta\alpha/(\beta\alpha+\alpha\beta)$ ratios and high relative abundances of C_{27} , C_{29} and C_{30} homologs relative to the extended C_{31} to C_{35} homohopanes (Table S3, Figs. S5C,D). An unusual elevated proportion of C_{27} – C_{30} hopanes in *Dickinsonia* and *Andiva* extracts, relative to bulk extracts from the Zimmie Gory and Lyamtsa localities, might indicate relatively large proportions of cyanobacteria among hopanoid-producing bacteria in the underlying microbial mats when compared to bulk organic matter. However, the unusual hopane pattern may also be the result of differences in the diagenesis of hopanoids between organic films and bulk samples (17).

Methylhopanes

The 2-methylhopane index (2-MHI) measures the abundance of C_{31} 2-methylhopane relative to C_{30} hopane (Table S3). 2-MHI is low and similar in all analysed fossils where 2-methylhopanes were detected (2-MHI = 0.8–1.8%). Elevated 2-MHI have been interpreted as an indicator for significant cyanobacterial contribution to sedimentary organic matter (50). However, only a minority of cyanobacteria have the ability to produce 2-methylhopanoids (51), and their content in cyanobacteria significantly depends on growth conditions (52). Apart from cyanobacteria, 2-methylhopanoids can also be produced by other oxygenic and anaerobic bacteria including alphaproteobacteria and an acidobacterium (51). Thus, in light of the unspecific taxonomic distribution of 2-methylhopanoids, and environmental control on their biosynthesis (51, 53), the 2-MHI values in the fossils do not yield any further insights about biological origins. 3β -methylhopanes were detected in small amounts in the samples (Table S3) and might reflect a minor contribution of methanotrophic bacteria to the organic matter of the samples (the 3-methylhopane index values 3-MHI = 1.1–2.6%) (54).

n-Alkanes and methylalkanes

Bulk extracts of background sediment from the Zimmie Gory and Lyamtsa localities demonstrate odd-over-even predominance among *n*-alkanes at all chain lengths and, unusually for the Precambrian, a relatively large proportion of long-chain *n*-alkanes with odd-over-even predominance (Figs. S5A,B). Such a distribution might indicate that a large proportion of *n*-alkanes is derived from cyanobacteria or green algae (17). All *Andiva* and the leanest *Dickinsonia* extracts do not provide sufficient signal for *n*-alkane analysis. The richest *Dickinsonia* extracts demonstrate the same *n*-alkane pattern as the background, however the fossil extracts additionally contain large proportions of short-chain (up to C_{19}) *n*-alkanes with no odd-over-even predominance (Fig. S5A). These *n*-alkanes are presumably directly derived from *Dickinsonia* or from degrading bacteria. However, such compounds are widely distributed in nature and do not provide any further phylogenetic information. All samples demonstrate only low amounts of methylalkanes, which likely represent diagenetic products of *n*-alkanes formed through clay mediated catalysis (55).

Other saturated and aromatic hydrocarbons

The majority of hydrocarbons extracted from the analysed samples are represented by *n*-alkanes, steranes and hopanes, with minor amounts of cheilanthanes, which are ubiquitous molecules of unknown origin. Aromatic compounds, apart from MAS and triaromatic steroids (TAS), include polycyclic aromatic hydrocarbons represented by typical parent and alkylated phenanthrenes and naphthalenes found in most bitumens and oils. TAS follow the patterns of distribution of MAS, demonstrating slightly lower relative content of cholesteroloids (e.g. in the richest *Dickinsonia*, cholesteroloid : ergosteroid : stigmasteroid abundances = 86% : 5% : 9%).

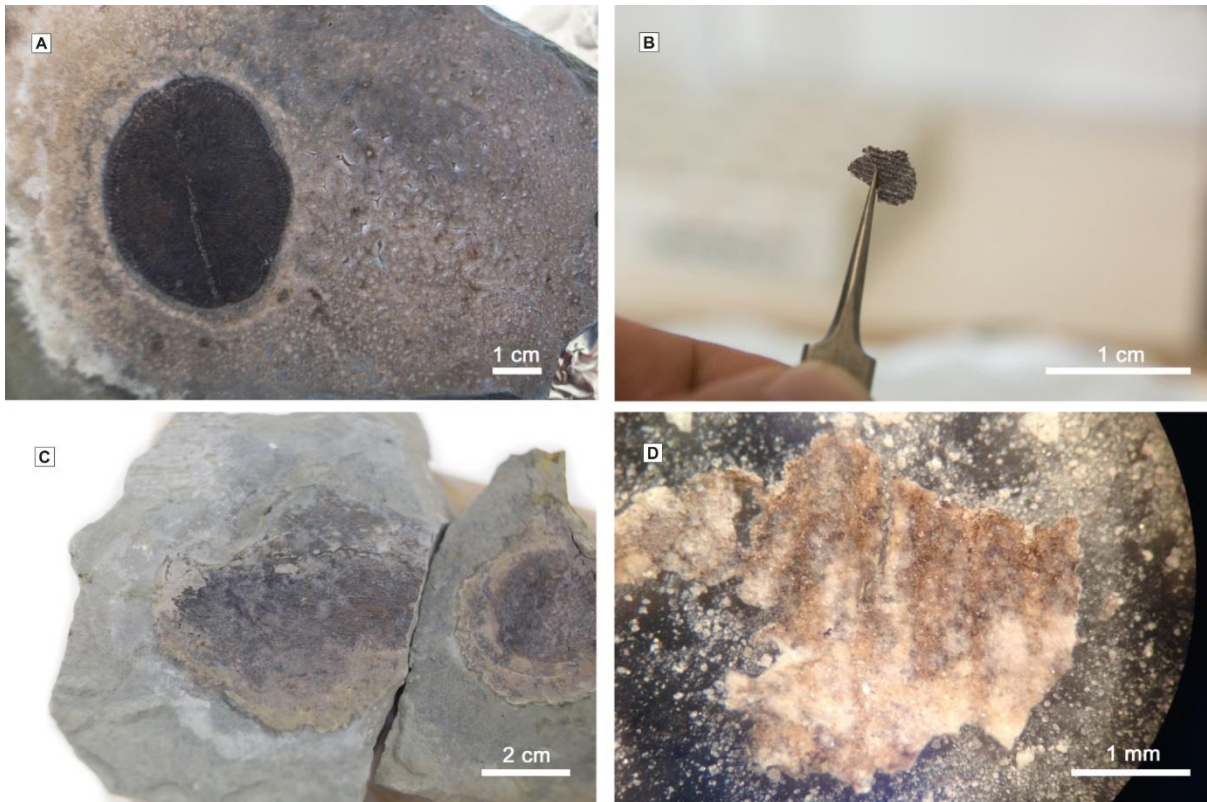
Syngeneity of biomarkers

GC-MS MRM, SIR and full-scan analyses of the comprehensive accumulatory laboratory system blank confirmed that the detected hydrocarbons were not introduced by laboratory processes. Monitoring of the blank yielded no *n*-alkanes, hopanes or steranes, even when measured using the most sensitive GC-MS MRM methods (Fig. S6). The only contaminants detected in the blank are trace amounts of phthalates—plasticizers present in small amounts in solvents used for extraction of biomarkers.

The results of Exterior/Interior (E/I) experiment, as well as a detailed discussion of biomarkers syngeneity of the samples from the White Sea that were collected, transported and stored in the same way as samples used in this study are presented elsewhere (17). The results show nearly identical concentrations of all biomarkers in exterior and interior rock portions with E/I = 1.09 to 1.53 for *n*-alkanes and E/I = 0.93 to 1.05 for hopanes and steranes, which indicates that the precombusted aluminium foil and clean calico bags prevented contamination of samples during transportation and storage, and confirm that all detected compounds are indigenous (17).

Dickinsoniid extracts demonstrate the same exceptionally low thermal maturity as *Beltanelliformis* and organically preserved macroalgae from the Lyamtsa locality (17). The high $\beta\alpha/(\beta\alpha + \alpha\beta)$ and low $Ts/(Ts + Tm)$ hopane isomer ratios, virtual absence of diasteranes and $\alpha\beta\beta$ sterane isomers, and presence of $\beta\alpha\alpha$ steranes (Fig. 1C; Table S3), which are only found in the most immature sediments, demonstrate that the hydrocarbons are significantly below the so-called oil-generative window, i.e. the kerogen never thermally generated and expelled liquid hydrocarbons (54). Such a low thermal maturity is never observed in contaminant petroleum products and migrated oils, which by their very nature must have a maturity within the oil generative window. Thus, contamination of the samples by petroleum products or by migrated hydrocarbons did evidently not occur.

Supplementary Figures



5

Fig. S1. Separation of organic matter from dickinsoniids. (A) Organically preserved *Dickinsonia* (specimen 4) after treatment with hydrochloric and hydrofluoric acids. Note the thin film of organic matter covering the surface with microbial mat impression surrounding the fossil; (B) a piece of organic matter of *Dickinsonia*-3 separated from the specimen with tweezers; (C) organically preserved *Andiva* (specimen *Andiva*-1) after treatment with hydrochloric and hydrofluoric acids, the organic matter is more visible as it starts separating from the rocky surface where the acids were applied; (D) organic matter of *Andiva*-1 suspended in water after separation from the specimen showing preservation of *Andiva*'s fine structure.

10

15

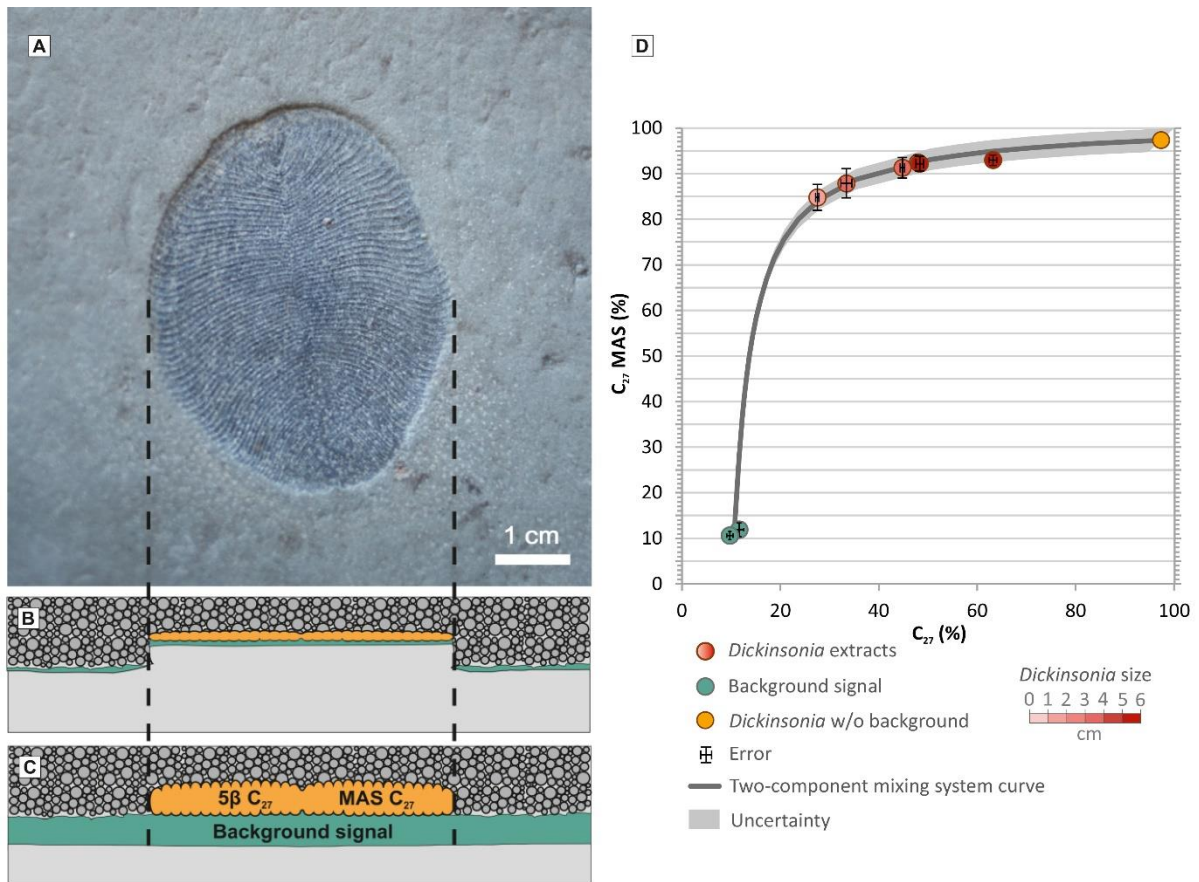
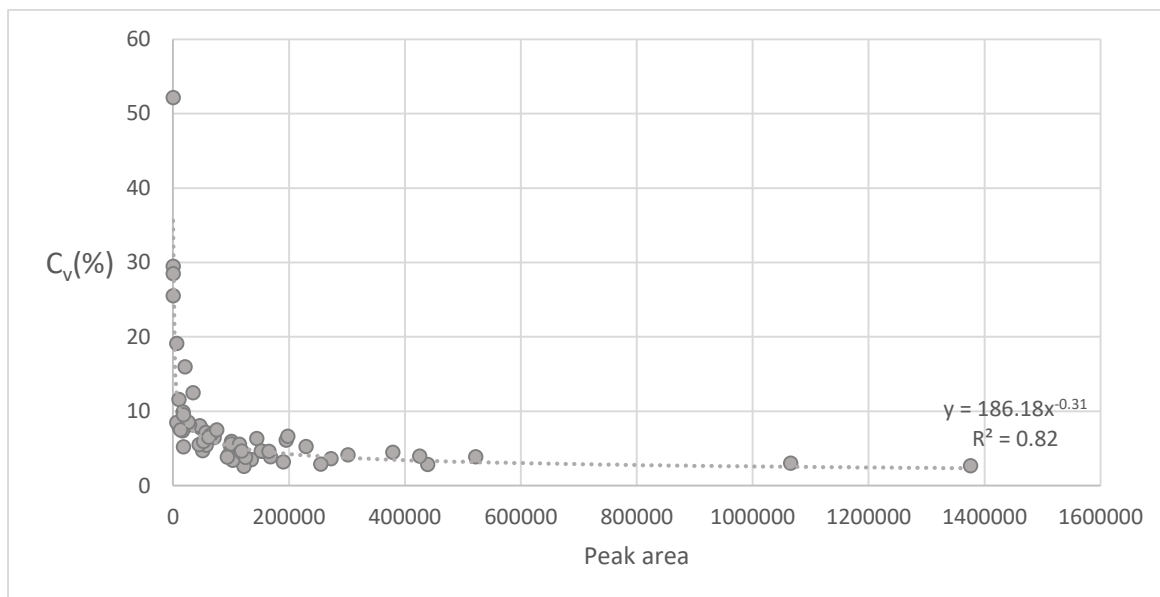


Fig. S2. Explanation of the origin of different biomarker signals of dickinsoniid extracts.

(A) Organically preserved *Dickinsonia* fossil (specimen 4) and surrounding impression of microbial mat; (B) schematic cross-section of the fossil, showing the position of organic matter of the microbial mat (green) and *Dickinsonia* (orange); (C) cross-section reconstructing the position of microbial mat and *Dickinsonia* immediately after burial beneath sand, highlighting the origin of the background signal in dickinsoniid extracts and explaining its variable influence depending on the size of a *Dickinsonia* specimen; (D) plot showing relationship between relative proportion of cholesteroloids among steranes (C_{27} (%)) and monoaromatic steroids (C_{27} MAS (%)); the dark-grey curve represents a numerically solved two component mixing scenario, and the light-grey area represent uncertainty of this curve (Supplementary Text).



5 **Fig. S3. Relationship between measured biomarker peak area and coefficient of**
variation (Cv). Each data point represents a different sterane or hopane in the AGSO-II
 industrial standard oil mixture, and the peak area is the dimensionless Metastable Reaction
 Monitoring (MRM) chromatographic signal area of the average of five repeat injections. Cv
 was computed for the ratio of compound signal area normalized to C₃₀ 17 α (H)21 β (H) hopane,
 which represents the highest signal in the MRM chromatograms. In the formula describing
 the relationship between measured biomarker peak area and Cv ($y = 186.18x^{-0.31}$), y = Cv, x =
 10 peak area.

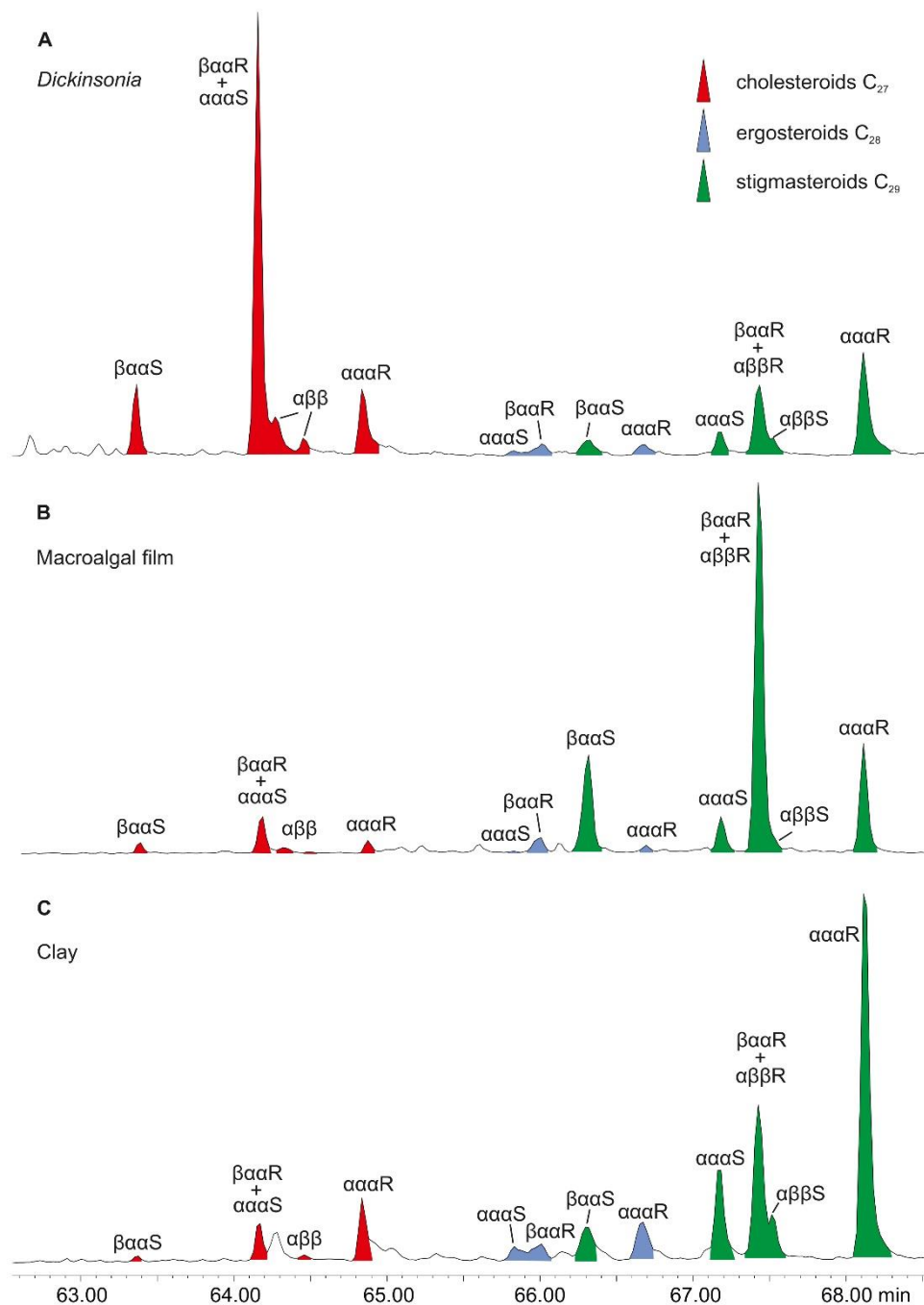


Fig. S4. Comparison of the sterane composition of *Dickinsonia-2* macroalgal film and background sediments from the Lyamtsa locality. (A) *Dickinsonia-2* displays elevated

5 **$5\beta/5\alpha = 5.5$ for cholestane only, while it is ~ 0.7 for ergostane and stigmastane; (B) the macroalgal film extract demonstrates elevated $5\beta/5\alpha$ ratios for all three steranes with $5\beta/5\alpha = 3.7$; (C) clay immediately underlying the level with *Dickinsonia* demonstrates typical background $5\beta/5\alpha$ ratio values of 0.64 for all three steranes. The elevated $5\beta/5\alpha$ ratios in the alga demonstrate that 5β steranes can form in sedimentary environments during decomposition of organic matter and that the process is not restricted to microbial activity**

10 **within the digestive system of animals (28) and is not caused by a specific nature of cholesteroloid in *Dickinsonia* and *Andiva*.**

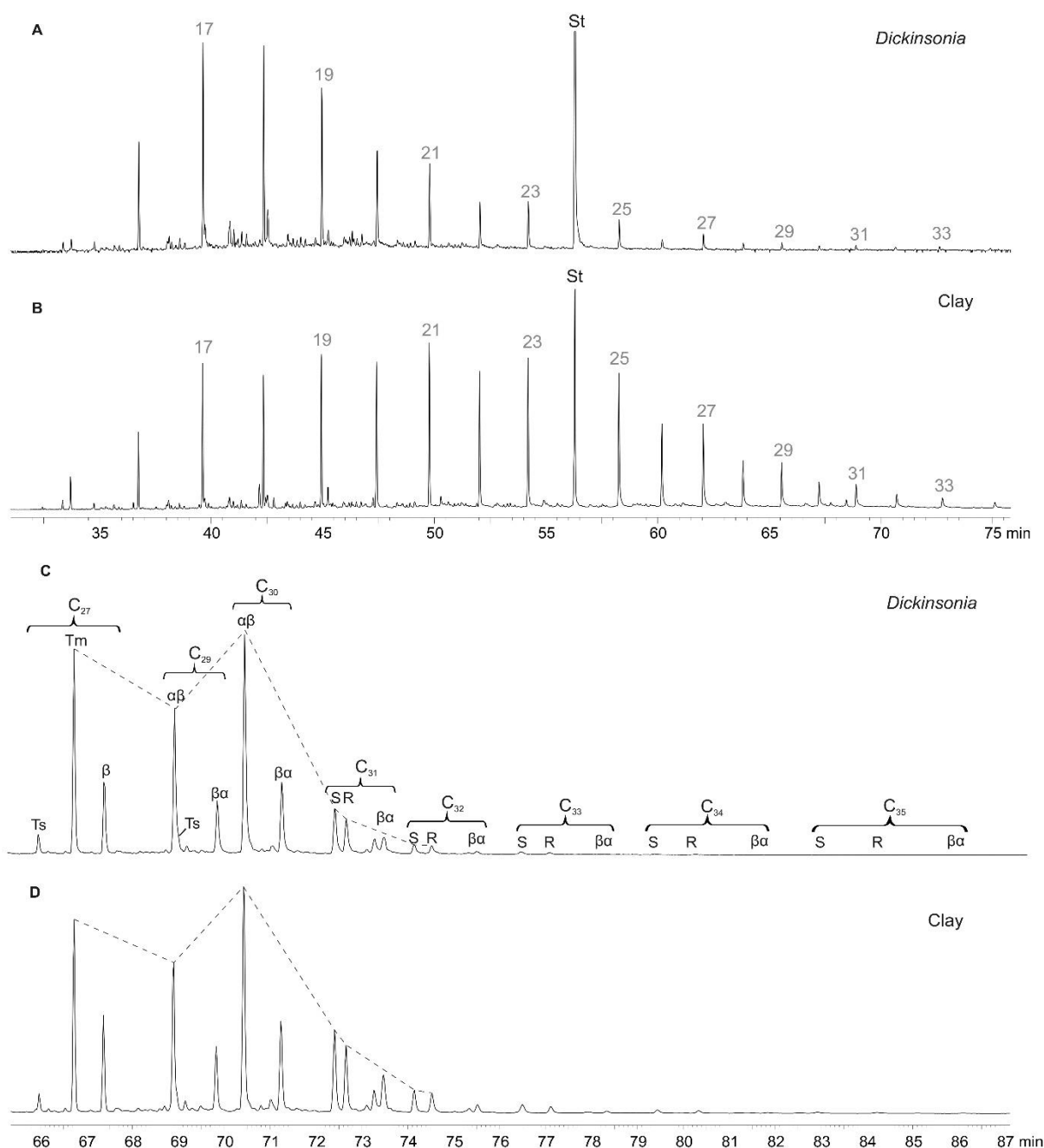


Fig. S5. Distribution of *n*-alkanes and hopanes in *Dickinsonia-2* and the underlying clay extracts. (A) Full-scan chromatogram, m/z 85 trace of *Dickinsonia-2* extract showing the distribution of *n*-alkanes; (B) full-scan chromatogram, m/z 85 trace of clay extract underneath *Dickinsonia* showing the distribution of *n*-alkanes; (C) Metastable Reaction Monitoring (MRM) chromatogram showing the sum of C_{27-35} hopane traces of *Dickinsonia-2* extract; (D) MRM chromatogram showing the sum of C_{27-35} hopane traces of clay extract. Numbers on chromatographic signals in (A) and (B) indicate the carbon number of *n*-alkanes, St = internal standard 18-MEAME. The dotted line in (C) and (D) highlights the difference in hopane (C_{27-30}) and homohopane (C_{31-35}) relative abundances between *Dickinsonia* and clay extracts. Hopane structures: $\alpha\beta = 17\alpha(H)21\beta(H)$, $\beta\alpha = 17\beta(H)21\alpha(H)$, S and R indicates stereochemistry at the C-22 position.

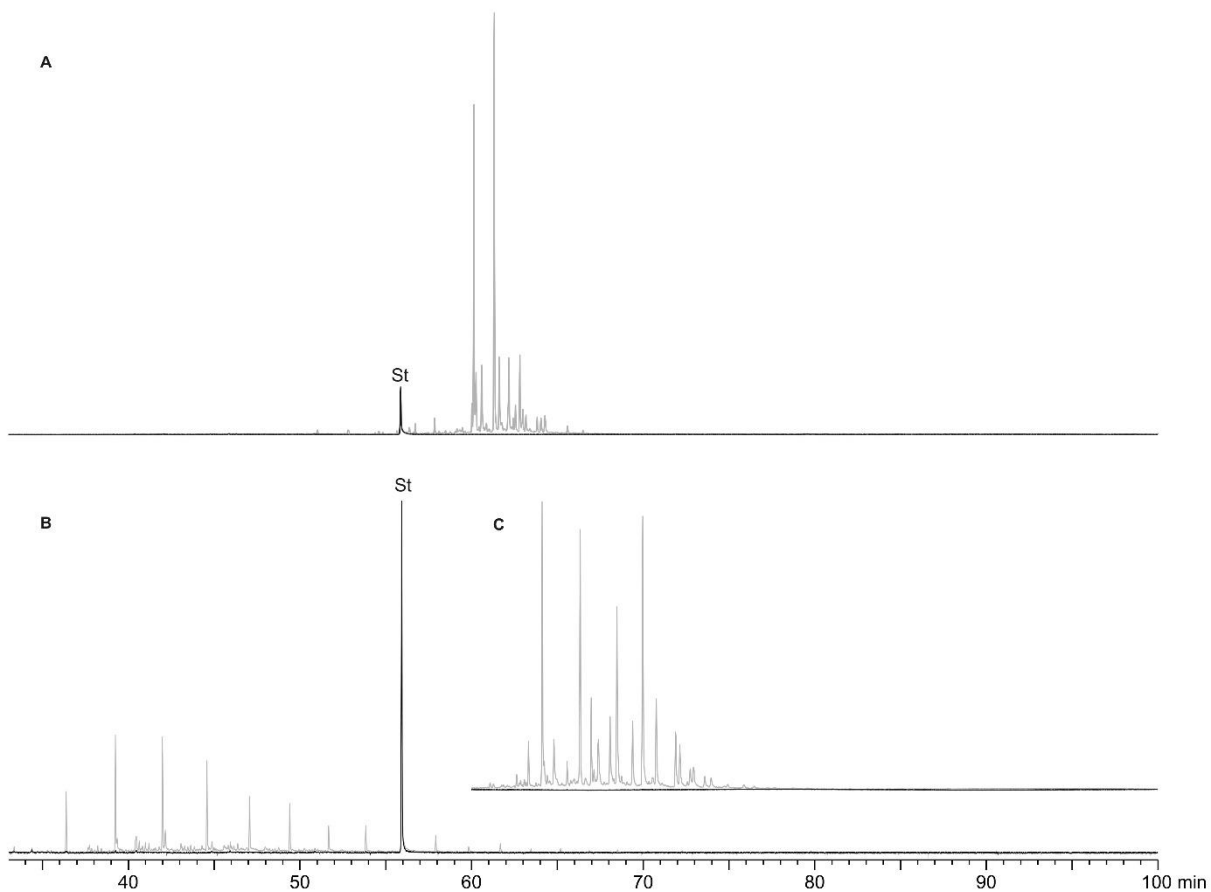


Fig. S6 | GC-MS chromatograms of a comprehensive accumulatory laboratory system blank (black line) in comparison to a *Dickinsonia-2* extract (grey line). (A) Selected Ion Recording (SIR) chromatogram showing monoaromatic steroids on mass trace m/z 253 ; (B) full-scan chromatogram m/z 85 trace (n -alkanes and methylalkanes); (C) Metastable Reaction Monitoring (MRM) chromatogram: $\Sigma(C_{27-35}$ hopanes, C_{27-29} steranes); St: 18-MEAME internal standard.

	MAS _y /H ¹			5β/5α ²		
	C ₂₇	C ₂₈	C ₂₉	C ₂₇	C ₂₈	C ₂₉
<i>Dickinsonia</i> -1	0.155 (0.004) ⁵	0.022 (0.001)	0.147 (0.003)	3.606 (0.207)	0.519 (0.324)	0.600 (0.057)
<i>Dickinsonia</i> -2	0.254 (0.005)	0.028 (0.001)	0.145 (0.004)	5.490 (0.28)	0.652 (0.231)	0.754 (0.056)
<i>Dickinsonia</i> -3	0.156 (0.004)	0.025 (0.001)	0.148 (0.004)	4.079 (0.29)	0.749 (0.265)	0.628 (0.043)
<i>Dickinsonia</i> -4	-	-	-	2.656 (0.408)	0.972 (0.344)	0.635 (0.08)
<i>Dickinsonia</i> -5	-	-	-	2.329 (0.102)	0.814 (0.288)	0.447 (0.019)
<i>Dickinsonia</i> -6	-	-	-	1.337 (0.071)	0.788 (0.279)	0.500 (0.022)
Variance (*10⁻⁴)³	32.617 (0.007)	0.076 (0.001)	0.024 (0.005)	21379 (4.4)	235 (5.038)	117 (0.878)
<i>Dickinsonia</i> sterol composition ⁴	99.70% (0.33)	0.23% (0.04)	0.07% (0.16)	98.38% (0.04)	1.08% (0.02)	0.54% (0.004)

Table S1. Estimation of the sterol composition of *Dickinsonia*.

- ¹ Concentration of C₂₇, C₂₈ and C₂₉ monoaromatic steroid (MAS) homologs (sum of isomers I and V) relative to total hopanes (sum of C₂₇–C₃₅ hopanes) in *Dickinsonia* extracts; hopanes: C₂₇ = Σ(Ts, Tm, β), C₂₉ = Σ(αβ, Ts, βα), C₃₀ = Σ(αβ, βα), C_{31–35} = Σ(αβ-22(S+R), βα), αβ = 17α(H)21β(H), βα = 17β(H)21α(H); y indicates carbon number of monoaromatic steroids; ²5β/5α = (βαα20R+ααα20S)/ααα20R; ³Variance = Σ(x - \bar{x})²/(n - 1), where x is C_y/H value, \bar{x} is a mean C_y/H value between the samples and n is the number of samples (n = 3); ⁴C_y% = 100%*(C_y variance)/(sum of variances for each of three steroids), y indicates carbon number of monoaromatic steroids; ⁵numbers in parentheses are standard deviation values.

	C ₂₇	C ₂₈	C ₂₉
<i>Andiva-1 5β/5α</i> ¹	1.072 (0.036) ⁴	0.758 (0.268)	0.685 (0.017)
<i>Andiva-2 5β/5α</i> ¹	1.315 (0.150)	0.811 (0.287)	0.517 (0.042)
<i>Andiva-Mat 5β/5α</i> ¹	0.805 (0.068)	0.761 (0.269)	0.65 (0.041)
Variance (*10⁻⁴)²	651.363 (1.192)	8.938 (3.369)	78.694 (0.432)
<i>Andiva</i> sterol composition³	88.14% ⁵ (0.46)	1.21% (0.46)	10.65% (0.08)

Table S2. Estimation of sterol composition of *Andiva*.

5 ¹5β/5α = (β α α 20R+ α α α 20S)/ α α α 20R; ²Variance = $\sum(x - \bar{x})^2 / (n - 1)$, where x is C_y/H value, \bar{x} is a mean 5β/5α value for each sterane between the samples and n is the number of samples ($n = 3$); ³C_y% = 100%*(C_y variance)/(sum of variances for each of three steroids); ⁴numbers in parentheses are standard deviation values; ⁵conservative minimum estimate of relative cholesterol content (C₂₇%) of *Andiva* (see Supplementary Text).

Sample	Ts/(Ts+Tm) C ₂₇ hopanes	β α /(β α + $\alpha\beta$) C ₃₀ hopanes	22S/22(S+R) C ₃₁ hopanes	C ₂₇₋₃₀ /C ₃₁ hopanes ¹	2-MHI (%) ²	3-MHI (%) ³	S/H ⁴
<i>Dickinsonia-1</i>	0.09 (0.01)	0.24 (0.01)	0.57 (0.01)	0.41 (0.01)	5.22 (0.03)	0.82 (0.08)	1.92 (0.16)
<i>Dickinsonia-2</i>	0.08 (0.00)	0.27 (0.01)	0.55 (0.01)	0.59 (0.01)	6.44 (0.03)	0.91 (0.09)	1.39 (0.13)
<i>Dickinsonia-3</i>	0.09 (0.01)	0.24 (0.01)	0.58 (0.01)	0.38 (0.01)	5.57 (0.03)	0.96 (0.11)	2.57 (0.24)
<i>Dickinsonia-4</i>	0.09 (0.01)	0.27 (0.03)	0.56 (0.03)	0.26 (0.01)	6.32 (0.06)	1.00 (0.22)	1.91 (0.34)
<i>Dickinsonia-5</i>	0.11 (0.01)	0.27 (0.02)	0.55 (0.02)	1.41 (0.04)	6.15 (0.06)	-	-
<i>Dickinsonia-6</i>	0.09 (0.01)	0.27 (0.02)	0.55 (0.02)	0.89 (0.02)	6.22 (0.05)	-	-
<i>Dickinsonia-7</i>	0.08 (0.02)	0.32 (0.06)	0.53 (0.06)	0.73 (0.05)	5.93 (0.12)	-	-
<i>Dickinsonia-8</i>	-	-	-	-	-	-	-
<i>Dickinsonia-Sandstone</i>	0.10 (0.00)	0.25 (0.01)	0.53 (0.01)	0.44 (0.01)	4.48 (0.02)	1.13 (0.07)	2.88 (0.15)
<i>Dickinsonia-Clay</i>	0.07 (0.00)	0.31 (0.01)	0.55 (0.02)	0.27 (0.00)	3.85 (0.87)	1.47 (0.07)	2.89 (0.13)
<i>Andiva-1</i>	0.03 (0.00)	0.31 (0.01)	0.38 (0.01)	0.17 (0.00)	3.82 (0.02)	0.95 (0.08)	1.34 (0.12)
<i>Andiva-2</i>	0.10 (0.01)	0.30 (0.03)	0.40 (0.03)	0.17 (0.01)	3.93 (0.05)	1.76 (0.27)	1.06 (0.21)
<i>Andiva Mat</i>	0.07 (0.01)	0.33 (0.03)	0.37 (0.03)	0.19 (0.01)	3.82 (0.05)	1.11 (0.21)	1.29 (0.26)
<i>Andiva-Sandstone</i>	0.04 (0.00)	0.37 (0.01)	0.39 (0.02)	0.24 (0.00)	5.63 (0.02)	0.80 (0.06)	0.93 (0.08)
<i>Andiva-Clay</i>	0.05 (0.00)	0.33 (0.01)	0.38 (0.01)	0.22 (0.00)	3.03 (0.02)	0.96 (0.05)	0.68 (0.04)

Table S3. Hopane and methylhopane biomarker parameters in extracts of dickinsoniids and surrounding deposits.

- 5 ¹C₂₇ = Σ (Ts, Tm, β), C₂₉ = Σ ($\alpha\beta$, Ts, $\beta\alpha$), C₃₀ hopane = Σ ($\alpha\beta$, $\beta\alpha$), C₃₁ = Σ ($\alpha\beta$ -22(S+R), $\beta\alpha$);
²2-methylhopane index, 2-MHI (%) = 100*(Σ C₃₁ 2 α +2 β -methylhopane)/ (Σ C₃₁ 2 α +2 β -methylhopane + Σ (C₃₀ $\alpha\beta$ -22(S+R), $\beta\alpha$ hopane); ³3-methylhopane index, 3-MHI (%) = 100*(Σ C₃₁ 3 β -methylhopane)/ (Σ C₃₁ 3 β -methylhopane + Σ ($\alpha\beta$ -22(S+R), $\beta\alpha$ C₃₀ hopane);
10 ⁴S/H = Σ (C₂₇₋₂₉ steranes)/ Σ (C₂₇₋₃₅ hopanes), steranes: C₂₇ = Σ ($\beta\alpha$ -20(S+R)-diacholestane, $\alpha\alpha\alpha$ - and $\beta\alpha\alpha$ -20(S+R)-cholestane), C₂₈ = Σ ($\beta\alpha$ -20(S+R)-diaergostane, $\alpha\alpha\alpha$ - and $\beta\alpha\alpha$ -20(S+R)-ergostane), C₂₉ = Σ ($\beta\alpha$ -20(S+R)-diastigmastane, $\alpha\alpha\alpha$ - and $\beta\alpha\alpha$ -20(S+R)-stigmastane), $\alpha\alpha\alpha$ = 5 α (H),14 α (H),17 α (H), $\beta\alpha\alpha$ = 5 β (H),14 α (H),17 α (H); hopanes: C₂₇ = Σ (Ts, Tm, β), C₂₉ = Σ ($\alpha\beta$, Ts, $\beta\alpha$), C₃₀ = Σ ($\alpha\beta$, $\beta\alpha$), C₃₁₋₃₅ = Σ ($\alpha\beta$ -22(S+R), $\beta\alpha$), $\alpha\beta$ = 17 α (H)21 β (H), $\beta\alpha$ = 17 β (H)21 α (H); ⁵numbers in parentheses are standard deviation values.

Species	Type	Sample Origin	C ₂₇ to C ₂₉ Sterols		
			C ₂₇ %	C ₂₈ %	C ₂₉ %
<i>Collodaria</i> SpB	Polycystinea (Radiolaria)	Mediterranean (Villefranche sur Mer)	75.38	16.10	8.52
<i>Collodaria</i> SpA	Polycystinea (Radiolaria)	Mediterranean (Villefranche sur Mer)	73.82	18.77	7.41
<i>Collodaria</i> SpC	Polycystinea (Radiolaria)	Mediterranean (Villefranche sur Mer)	75.70	15.17	9.13
<i>Collodaria</i> SC2	Polycystinea (Radiolaria)	Mediterranean (Villefranche sur Mer)	60.54	23.30	16.16
<i>Collodaria</i> SC1	Polycystinea (Radiolaria)	Mediterranean (Villefranche sur Mer)	61.86	14.50	23.64
<i>A. lobifera</i>	Foraminifera	Red Sea (Eilat)	13.58	43.16	43.26
<i>Sorites</i> sp.	Foraminifera	Red Sea (Eilat)	30.67	20.06	49.27
<i>Shepherdella</i> sp.	Foraminifera	Red Sea (Eilat)	45.72	16.16	38.12
<i>Quinqueloculina</i> sp.	Foraminifera	Mediterranean (Tel Aviv)	78.15	14.66	7.19
<i>Acantharea</i> sp.	Acantharea	Indian Ocean near Eden	51.98	39.35	8.67
<i>Gromia</i> sp.	Gromiidae	Southern Ocean (McMurdo Sound)	11.77	27.88	60.35
<i>A. laticollaris</i> ¹	Foraminifera	Literature (31)	10.31	26.93	62.76

Table S4. Distribution of C₂₇-C₂₉ sterols in extant Rhizaria (Retaria and Gromiidae)

¹Values for *A. laticollaris* were determined by integrating peak areas of the functionalized sterols in Fig.1a of Grabenstatter et al. (31).